Local Velocity and Porosity Measurements Inside Casper Sandstone Using MRI

Melissa Robinson Merrill
Chemical Engineering Dept., University of Wyoming, Laramie, WY 82071

Magnetic resonance imaging is used to make nondestructive experimental measurements of fluid flow velocity and rock porosity inside a brine-filled Casper sandstone sample during brine injection. Two-dimensional images of these values are obtained in arbitrary cross sections, with pixel sizes on the order of 1 mm^2. The data are then statistically analyzed to find the variation of the average interstitial velocity as a function of porosity, as well as frequency distributions for both the velocity and porosity. The results show that as local porosity increases, the local flow velocity increases, according to the empirical relationship, $V = 0.0669\,\phi + 0.0055$. Thus, higher porosity regions of the core are better contacted by the displacement fluid. Results also imply bypassing of fluid around the perimeter of the core, indicating the need for a coreholder capable of sustaining higher overburden pressures on the order of 225 psi (1.55 MPa).

Introduction

In the petroleum industry there is a general belief that there must be a correlation between porosity and permeability in oilfield cores. This has been supported by porosity-permeability data obtained from core plugs, and generally relationships of the form

$$k = Ab^{\phi} \tag{1}$$

or

$$k = C\phi^{d} \tag{2}$$

have been proposed (Jorden and Campbell, 1984). Theoretical models suggest that the form of Eq. 2 is more applicable. Until recently, experimental evaluation of Eqs. 1 and 2 could be quite laborious, requiring measurements of porosity and permeability on large numbers of core plugs from a particular reservoir. But now, with the advent of magnetic resonance imaging (MRI) techniques for noninvasively measuring fluid flow velocities and porosities inside oil cores, it is possible to study quantitative relationships between local porosity and fluid flow velocity within a single core sample. Since velocity and permeability are related through Darcy's law, these results could eventually be used to evaluate Eqs. 1 and 2. Preliminary experiments have been performed on a Casper sandstone sample.

Casper sandstone has a porosity of 16–21% and a permeability of about 77–88 md (Leimkuhler, 1987). It is homogeneous on a large scale, although it contains layers of varying porosity and permeability which are apparent in the images. The core was cut so that the bulk flow would be roughly parallel to the layers. The presence of layers in the core suggests that fluid displacement experiments will show preferential channeling into high-permeability layers.

In this study, MRI is used to obtain fluid velocities in Casper sandstone during brine injection into a brine-filled core. A 2-D image of the interstitial water velocity is obtained in arbitrary cross sections, with pixel sizes on the order of 1 mm^2. Porosity values are also obtained in the same cross sections. The data are then statistically analyzed to find the variation of the average interstitial velocity as a function of porosity. The results show that as local porosity increases, the local flow velocity increases. Thus, higher porosity regions of the core are better contacted by the displacement fluid.

Using MRI to measure fluid velocities inside cores is extremely difficult. Because of high mineral content and high surface-to-volume ratios inside the cores, the T_2 relaxation constant is quite short (approximately 6 ms for Casper sandstone). To measure velocities accurately, pulse sequences with very short spin-echo times are required. In addition, the signal-to-noise ratio for core imaging experiments is only on the order of 10:1. Unless the flow rate is quite high inside the core, the

effect of the signal-to-noise ratio on the accuracy of the velocity measurement can be significant. Because of these conditions, long experiments are required to get adequate signal-to-noise by signal averaging. In this study, a modified 3-D FT (three-dimensional Fourier transform) pulse sequence is used to obtain the shortest echo times possible and yet have a sufficiently long flow encode time to measure the slow velocities observed in coreflood experiments.

Only axial flow was measured in this work. However, by varying the direction of the flow encode gradients, the same pulse sequence can be used to measure the other two orthogonal flow components and thus obtain the entire velocity vector for each point in the core.

Experimental Procedure

The experiments were conducted using a General Electric CSI *Omega* 2-Tesla imager with a 31 cm magnet bore. The system is equipped with *Acustar* actively-shielded gradient coils with strengths of up to 20 G/cm. The use of shielded gradients is recommended, because they elicit smaller eddy currents, thus improving the accuracy of the flow measurements. A 10.8 cm bird-cage RF coil tuned to protons (85 MHz) was used. Bird-cage coils are preferable, because they yield images with less intensity artifacts due to RF inhomogeneity (Hayes et al., 1985). The 90° pulse was 47 μs, and the 180° pulse was 94 μs.

A sample of Casper sandstone was used in these experiments. It had a diameter of 62.5 mm, a length of 116 mm, an average porosity of 21% (determined in the lab by measuring the mass of fluid required to saturate the core), and an estimated permeability of about 80 md (based on the range of permeabilities measured by Leimkuhler). It was cored with its axis approximately parallel to the bedding planes in the sample.

A modified Hassler-type coreholder was built for the flow experiments. This coreholder was specially designed for use in the imager and had no metal parts which might interfere with the RF signals or cause inhomogeneities in the magnetic field. A diagram of the coreholder is shown in Figure 1. It is composed of a 3 in. (76 mm) PVC pipe with two plexiglass end caps. The caps are held in place by eight Delrin rods with nylon washers and nuts. A cylindrical piece of rubber is placed inside the PVC pipe and wrapped around the ends, and a vacuum is used to pull the rubber against the PVC pipe. The core and Lucite spacers are placed inside the sleeve, and the end caps are positioned on the Delrin rods and tightened down. The vacuum is removed, and nitrogen gas at a pressure of about 120 psi (830 kPa) is forced into the annulus between the rubber and the PVC. It is this overburden pressure of nitrogen which is used to help prevent bypassing of the fluid around the perimeter of the core. The coreholder is unable to withstand higher pressures, and thus, some degree of bypassing was observed since the upstream pressure was close to 100 psi (690 kPa).

The core was vacuum-saturated before being placed inside the coreholder. First, the dry, clean core was placed in a vacuum chamber for 24 hours to remove all the air from the pore spaces. Then, while still under vacuum, a 1% KCl solution was introduced into the vacuum chamber until it covered the core. The core and KCl solution were left in the vacuum for four hours, and then they were returned to atmospheric pressure. KCl solution was used because a small clay content was suspected, and using distilled water could have swelled the clays, reducing the permeability of the core.

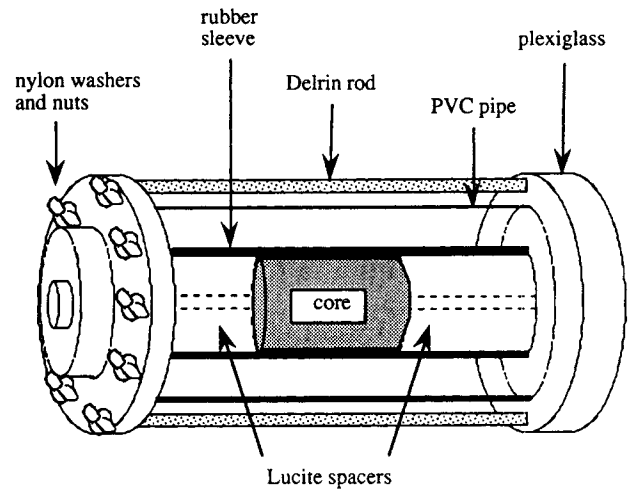

Figure 1. Hassler core holder.

Following vacuum saturation of the core, it was placed in the Hassler coreholder. The KCl solution was then injected into the core for 12 hours to ensure that the core was completely saturated prior to imaging. The porosity images do not show any regions of low or no porosity (porosity less than about 10%), indicative of air in the core, so it was concluded that the core was well saturated with the KCl solution. A very high flow rate of 2,300 cm^3/h was used to minimize the effects of noise on the velocity measurements.

A 3-D FT pulse sequence was modified to acquire the MRI data (Robinson, 1992). A diagram of the sequence is shown in Figure 2. It employs a conventional 3-D spin-echo pulse sequence, with the addition of flow encode gradients (GF in Figure 2) for measurement of the flow velocities.

The benefit of using a 3-D FT pulse sequence is that it uses a second-phase encode gradient for slice selection, instead of a slice selective gradient. Because this gradient can be applied simultaneously with the other phase encode gradient and a hard 90° pulse can be used, the length of the echo time is minimized. Minimizing the echo time is tantamount to maximizing the signal obtained.

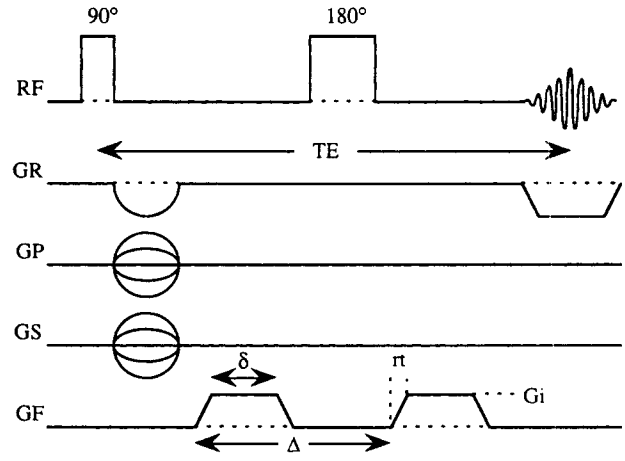

Figure 2. 3-D FT flow pulse sequence.

Table 1. Flow Imaging Parameters

	Velocity	Porosity
Number of averages	32	8
Recycle time (s)	0.40	2.0
Number of slices	16	16
Axial field of view (mm)	128	128
Image field of view (mm)	64	64
Image matrix size	64×64	64×64
Echo time (ms)	15	1.5
Flow gradient (G/cm)	−9.8, 0, +9.8	0
δ (ms)	6.477	0
r_t (ms)	0.175	0.175
Δ (ms)	7.025	0

The flow encode gradient lobes are positioned on each side of the 180° pulse, thus maximizing the flow encode time while minimizing the echo time. Such a configuration requires a very accurate 180° pulse, so that the total area of the flow encode gradients is zero. Small errors in the 180° pulse were corrected by adjusting the magnitude of the second lobe of the flow encode gradient. The parameters for the velocity measurements are shown in Table 1.

For the measurement of the porosities, the same pulse sequence in Figure 2 was used, with the flow encode gradients set to zero. The values of the parameters are shown in Table 1.

Theory

Porosity measurements

The magnitude of the signal obtained using a 3-D FT pulse sequence is directly proportional to the amount of water contained in the image voxel. The average values of the porosity in each voxel were calculated by dividing the magnitude of the signal by a constant, so that the average porosity for the core would be equal to the value of 21% measured in the lab by weighing. The method assumes a fairly homogeneous core, so that a subregion of the porosity (a slice) equals the porosity of the entire core sample. The method is valid only if the echo time is small enough not to lose signal due to T_2 relaxation. It assumes that there is only a single T_2 relaxation time for the entire core, which may not always be valid. For this core, however, it was found that the T_2 data could be represented by a single exponential function, and that using a single T_2 value did not cause a significant error in the measurement of accurate porosities (Merrill, 1994).

Velocity measurements

The velocity of the flow is measured in terms of the phase of the transverse spin magnetization. The phase shift (φ) in a voxel due to fluid moving with a constant velocity component V_i in the i coordinate direction is (Hahn, 1960):

$$\varphi = \gamma m_1 V_i, \tag{3}$$

where m_1 is the first moment of the gradient,

$$m_1 = \int t G_i(t)\, dt. \tag{4}$$

For the bipolar, trapezoidal gradients used in these experiments, Eq. 3 simplifies to:

$$\varphi = \gamma G_i \Delta (\delta + r_t) V_i, \tag{5}$$

where Δ is the time separating the gradient pulses, r_t is the ramp time of the gradient pulse, δ is the duration of the pulse, and G_i is the magnitude of the pulse (see Figure 2).

Differentiating Eq. 5 with respect to G_i, we obtain:

$$(d\varphi/dG_i) = \gamma \Delta (\delta + r_t) V_i. \tag{6}$$

Therefore, the velocity in a voxel is directly proportional to the slope of the line resulting from a graph of φ vs. G_i. In our experiments, we determined this slope from the observed phase at three different values of G_i: −9.8 G/cm, 0 G/cm, and +9.8 G/cm. Using a linear regression to obtain the velocity should be more accurate than measuring the phase shift at only one value of the gradient, since it helps to cancel out noise effects.

Unfortunately, one cannot simply image the flow and obtain the phase shift directly from the data. Because of eddy currents and other effects, one must have baseline data to use as a reference for the given phase. For that reason, two data sets were obtained for every value of the flow encode gradient: one with no flow going through the core and the second with the flow turned on. The phase difference between the two images was used as φ in Eq. 6.

It is possible to obtain all three components of the velocity vector by performing three experiments using three orthogonal gradients to flow encode the x-, y- and z-directional flow. However, only z-directional (axial) flow was measured in this study.

Experimental Results

Figure 3 shows images of the porosity and positive and negative flow velocities for eight image slices through the Casper sandstone core. The image slices are shown perpendicular to the direction of flow.

The images of the porosity show evidence of the bedding planes in the core, as seen by the variations in the grey scale of the image. If one makes a frequency distribution of the porosity data for the eight slices (porosity distribution), Figure 4 is obtained. It indicates that the porosity does not have a normal distribution, but can be modeled very nicely using a bimodal Gaussian distribution, where 60% of the core has an average porosity of 0.221, and 40% of the core has an average porosity of 0.185. It is believed that the two values of the porosity correspond to two different types of bedding planes in the core.

The flow images indicate that the bulk of the flow is in the positive direction, with some negative flow apparent only at the edges of the core. The negative flow velocities have two sources. The scattering of negative velocities within the core is most likely caused by noise in the data. The negative flow apparent at the perimeter of the core is most likely caused by bypassing of the fluid around the core. Such bypassing can have a high velocity; however, the phase is constrained to fall between $-\pi$ and $+\pi$. Thus, high velocity can appear as negative velocity if a phase wrap occurs, causing a phase greater than $+\pi$ to be measured as a value less than zero.

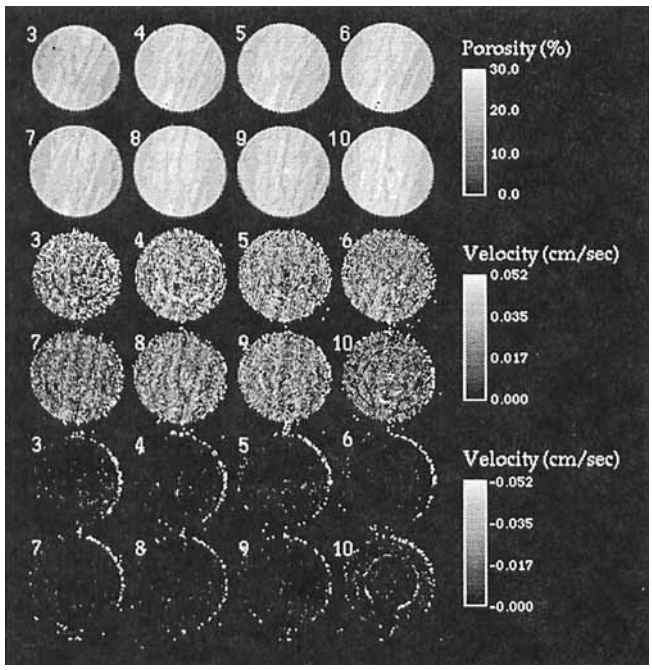

Figure 3. Casper sandstone: measurement of flow velocities.

The flow in the positive direction appears to be fairly uniform. The flow distributor is faintly visible in slice 10, so this slice was not used in any of the following calculations.

For each value of the porosity (rounded to the nearest whole number), the velocity was determined from the MRI data. A running sum of the velocities was kept, and then the average velocity was calculated by dividing the sum of the velocities by the number of points at a particular value of the porosity.

The data obtained from this calculation are shown in Figure 5, in which the average velocity vs. porosity is superimposed on the porosity distribution. The data indicate that as the local porosity increases, the average velocity through the voxel also

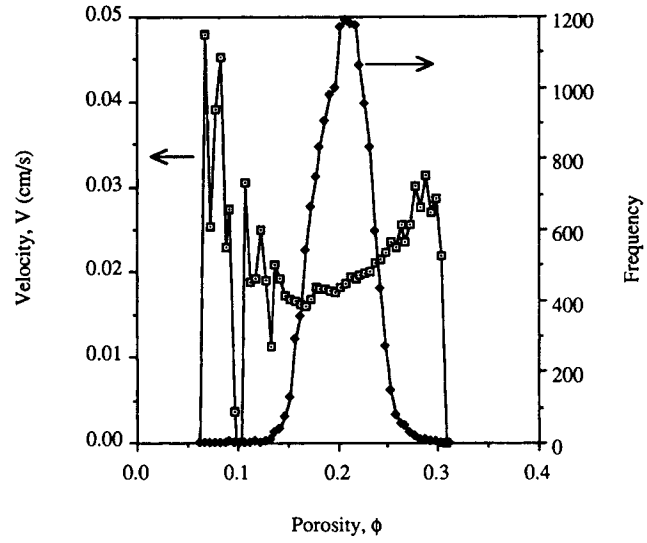

Figure 5. Velocity as a function of porosity.

increases. This supports the assumption that as porosity increases, permeability also increases. An empirical equation relating velocity and porosity could be developed from the data and used in coreflood simulation programs. A straight line fit to the data (ignoring points where the porosity distribution shows fewer than 50 data points) gives the relationship:

$$V = 0.0669\phi + 0.0055 \tag{7}$$

where V is the velocity in cm/s, and ϕ is the porosity as pore volume percent. The fit is shown in Figure 6 and has an r^2 value of 0.882.

Figure 7 shows a histogram of the velocities for the core (velocity distribution). A Gaussian distribution is superimposed on the data. The distribution appears to be fairly normal. This is surprising, considering the fact that the porosity data was bimodal and Eq. 7 predicts a linear relationship between porosity and velocity. The most likely explanation is that noise

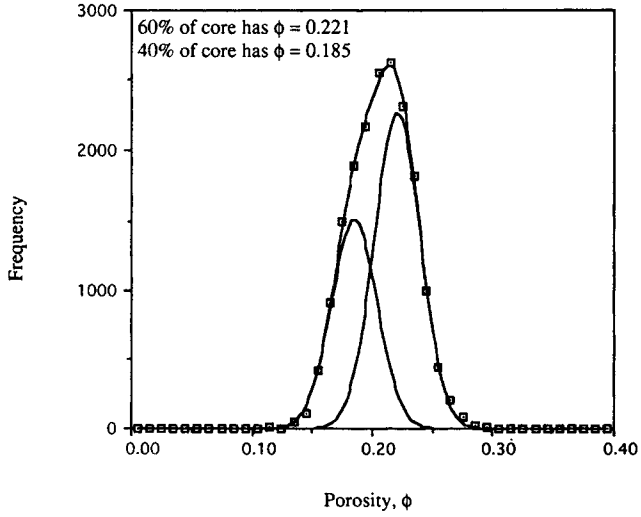

Figure 4. Bimodal porosity distribution for Casper sandstone.

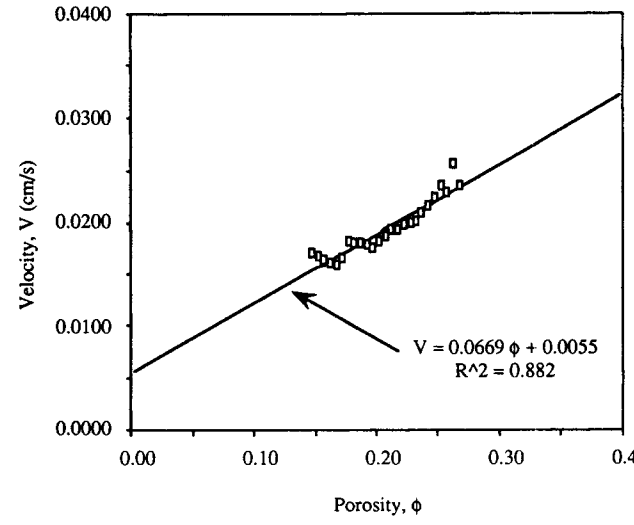

Figure 6. Empirical fit to velocity-porosity data.

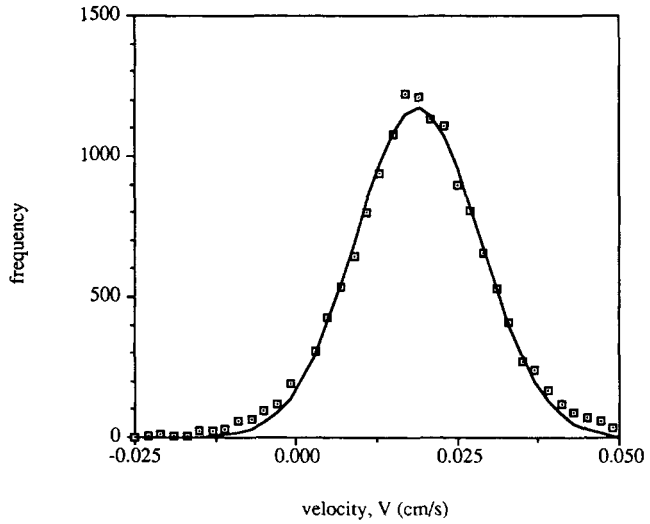

Figure 7. Histogram of velocities for Casper sandstone.

in the velocity data obscures the bimodal characteristics of the distribution.

An average velocity of 0.0189 cm/s was calculated from the MRI data, using

$$\langle V \rangle = \frac{\Sigma V_{i,j} \phi_{i,j} A_{i,j}}{\Sigma V_{i,j} A_{i,j}} \tag{8}$$

This number is much smaller than the average interstitial velocity calculated using the flow rate of 2,300 cm^3/h (which gives a velocity of 0.10 cm/s). The most likely explanation is that bypassing of the fluid occurred in a thin film around the outside of the core. This is possible, because the overburden pressure differential on the rubber sleeve was only about 20 psi (138 kPa). Figure 8 shows the results of using a projection of the data to obtain the average velocity through the core for a number of different overburden pressures. The figure indicates that the actual flow going through the core remains relatively constant as the overburden pressure is decreased. This suggests that as the overburden pressure is reduced, the amount of fluid contacting the core remains stable, while the amount of fluid bypassing the core continuously increases. The experiments indicate that quantitative measurements of the velocity can be made, provided that the overburden pressure is at least 125 psi (861 kPa). For higher flow velocities, it is expected that an even higher overburden pressure would be required. For the flow rate of 2,300 cm^3/h, the upstream pressure was 100 psi (690 kPa), indicating that a coreholder capable of handling at least 225 psi (1.55 MPa) total pressure is required.

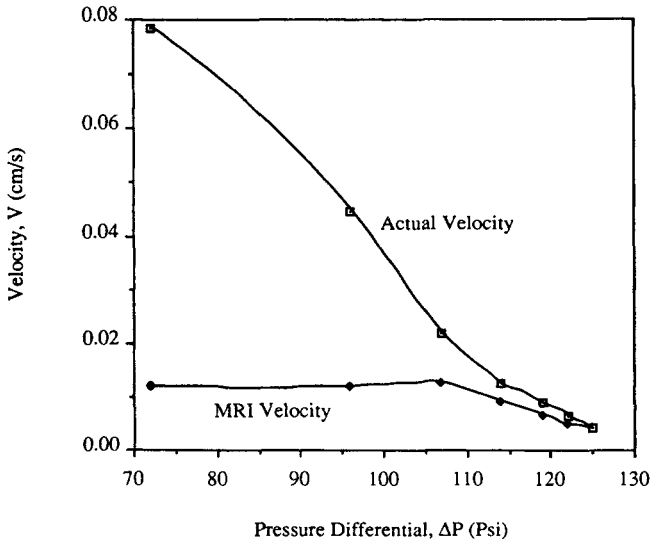

Figure 8. Effect of bypassing.

Conclusions

Local flow velocities and local porosities have been measured on a sample of Casper sandstone using MRI. Qualitative images of the porosities show evidence of bedding planes in the core. A bimodal fit to the porosity distribution indicates two types of layers in the core with average porosities of 0.221 and 0.185. The images of the velocity show that the bulk of the flow is in the same direction as the applied pressure gradient, with a small number of points at the edge of the core having an apparent velocity in the opposite direction. The images of negative flow velocities indicate that bypassing may be occurring in a thin film around the perimeter of the core. A substantial overburden pressure [at least 125 psi (861 kPa)] is needed to prevent this bypassing. A velocity distribution has been plotted for the core, which has a Gaussian shape.

The relationship between average velocity and porosity indicates that local velocity increases with an increase in local porosity. A straight line was used to obtain an empirical relationship between average velocity and porosity in this core sample. The difference between calculated average velocity based on flow rate and average velocity measured by MRI may be due to bypassing. A much higher overburden pressure is recommended to prevent bypassing of the fluid around the outside of the core. Further experiments should be performed to assess the quantitative limits of MRI measurements of flow velocities.

Acknowledgment

The author would like to thank Dominic Palese for building the coreholder used in the experiments and Zhisong Jin for writing the computer code for processing the data. Yashwant Wagle is gratefully acknowledged for his contributions to this article.

Notation

G_i = gradient applied in the i coordinate direction
m_1 = first moment of the flow gradient
r_t = gradient ramp time
t = time
V = velocity
V_i = velocity in the i coordinate direction

Greek letters

γ = gyromagnetic ratio (4,260 Hz/G for ^1H)
δ = flow encode gradient duration
Δ = time separating flow encode pulses
φ = phase shift in a voxel due to flow
ϕ = porosity

Literature Cited

Hahn, E. L., "Detection of Sea-Water Motion by Nuclear Precession," *J. Geophys. Res.*, **65**, 776 (1960).

Hayes, C. E., W. A. Edelstein, J. F. Schenck, O. M. Mueller, and M. Eash, "An Efficient, Highly Homogeneous Radiofrequency Coil for Whole-Body NMR Imaging at 1.5 T," *J. Magn. Reson.*, **63**, 622 (1985).

Jorden, J. R., and F. L. Campbell, *Well Logging I: Rock Properties, Borehole Environment, Mud and Temperature Logging*, SPE Monograph, Vol. 9, Soc. of Petr. Engrs. of AIME, Dallas (1984).

Leimkuhler, J. M., "Changes in Sandstone Permeability Induced by Completion Fluid Invasion," MS Thesis, Univ. of Wyoming (1987).

Merrill, M. R., "Porosity Measurements in Natural Porous Rocks Using Magnetic Resonance Imaging," *Appl. Magn. Reson.*, **5**, 307 (1994).

Robinson, M. A., "Measurement of Fluid Velocities During Water Injection Into Natural Porous Rocks," SPE 24369, SPE Meeting, Casper, WY (May 18-21, 1992).

Manuscript received May 12, 1993, and revision received Oct. 12, 1993.